Advances in Water Resources 130 (2019) 29–36

Contents lists available at ScienceDirect

Advances in Water Resources

journal homepage: www.elsevier.com/locate/advwatres

Two-site colloid transport with reversible and irreversible attachment: Analytical solutions

Vasileios E. Katzourakis, Constantinos V. Chrysikopoulos*

School of Environmental Engineering, Technical University of Crete, Chania 73100, Greece

ARTICLE INFO

Keywords:
Transport
Reversible attachment
Irreversible attachment
Porous media
Mathematical modeling

ABSTRACT

Analytical solutions for colloid transport in water saturated, one-dimensional, homogeneous porous media, under fully developed uniform flow are presented. The colloids can be either suspended in the aqueous phase or attached reversibly and/or irreversibly onto the solid matrix. Both attachment rates are assumed linear, and any possible blocking or ripening effects are neglected. The colloids can be either of neutral density or denser than the water. For dense colloids, gravity effects are accounted for. Gravity may enhance or hinder the migration of dense colloids, depending on the flow direction. Upstream boundary conditions for both instantaneous and broad-pulse colloid injections are accounted for. The new analytical solutions were used to successfully fit available experimental data.

1. Introduction

Colloid particle migration in water saturated subsurface formations is of great importance to several scientists and environmental engineers. The transport of colloids in water saturated formations is influenced by a number of factors including water velocity, ionic strength, pH, solution chemistry, formation type, density and size of particles (Chrysikopoulos and Katzourakis, 2015; Scholl and Harvey, 1992; Shellenberger and Logan, 2002). In case of biocolloids (bacteria, viruses) additional factors such as growth, chemotaxis and decay may also affect transport behavior (Ginn et al., 2002). Dense particles can be affected by gravity (Chrysikopoulos and Syngouna, 2014; Flowers and Hunt, 2007; James and Chrysikopoulos, 2003; Katzourakis and Chrysikopoulos, 2015), which may hinder or enhance their transport depending on the flow direction.

The flow direction in typical bench-scale flow-through experiments can be either upward to minimize air entrapment (Keller et al., 2004; Tan et al., 1994; Tong and Johnson, 2007), downward (Saiers et al., 1994; Syngouna and Chrysikopoulos, 2015; Xu et al., 2006) or horizontal (Lee and Chrysikopoulos, 2002; Syngouna et al., 2017), which is representative of natural systems. Unfortunately, the importance of flow direction in experimental studies is not always taken into account and some studies neglect to report it, assuming that gravity and hydrodynamic effects are negligible (Basha and Culligan, 2010). However, Syngouna and Chrysikopoulos (2016) reported that the attachment of viruses onto colloids was higher for downward flow rather than upward flow direction. Similarly, Basha and Culligan (2010) observed that particle deposition was greater for upward flows rather than for downward flows, suggesting that gravity clearly influences particle transport.

There are several models published in the literature that combine the classical advection-dispersion equation with different types of kinetic attachment models. Most of these transport models assume that attachment follows either one-site kinetics with forward and reverse terms or two-site kinetics with reversible and irreversible attachment. The forward rate of reversible attachment may represent deposition in secondary minimum ("fast" deposition), while the forward rate of irreversible attachment may represent deposition in primary minimum ("slow" deposition) (Tufenkji and Elimelech, 2005). The two-site kinetics model has been employed in various studies (Basha and Culligan, 2010; Compère et al., 2001; Harvey and Garabedlan, 1991; Schijven et al., 2002; Tong and Johnson, 2006; Yoon et al., 2006). There are several one- and three-dimensional, analytical or numerical models for colloid or biocolloid transport in literature (Anders and Chrysikopoulos, 2009; Bradford et al., 2011; Harvey and Garabedlan, 1991; Park et al., 1992; Sim and Chrysikopoulos, 1996). Furthermore, two-site models which combine equilibrium and non-equilibrium kinetic sorption (Cameron and Klute, 1977) with two-region models (Van Genuchten and Wagenet, 1989) that capture physical and chemichal non-equilibrium processes have been published in the literature. These models have been incorported in the software Stanmod (Simunek et al., 1999; van Genuchten et al., 2012). Though there is a rather limited collection of mathematical models dealing with dense colloid transport (Flowers and Hunt, 2007; Chrysikopoulos and Syngouna, 2014; Katzourakis and Chrysikopoulos, 2015) and even a narrower collection of analytical

* Corresponding author.
E-mail address: cvc@enveng.tuc.gr (C.V. Chrysikopoulos).

https://doi.org/10.1016/j.advwatres.2019.05.026
Received 3 February 2019; Received in revised form 29 May 2019; Accepted 30 May 2019
Available online 31 May 2019

Nomenclature

A	variable defined in Eq. (13), 1/t.
A_c	cross-sectional area of the porous medium (column), L^2.
B	variable defined in Eq. (14), 1/t.
b	ratio of average free settling segment length to the grain radius, (–).
C_c	concentration of suspended colloids, M_c/L^3.
C_{c_0}	constant injected concentration of suspended colloid particles, M_c/L^3.
C_{c^*}	concentration of colloids attached onto the solid matrix, M_c/M_s.
$C_{c*}^{(i)}$	concentration of colloids irreversibly attached onto the solid matrix, M_c/M_s.
$C_{c*}^{(r)}$	concentration of colloids reversibly attached onto the solid matrix, M_c/M_s.
d_p	colloid particle diameter, L.
D_c	hydrodynamic dispersion coefficient of colloids, L^2/t.
erfc	complementary error function.
f_s	settling velocity correction factor, (–).
g	gravitational acceleration, L/t^2.
g_x	gravitational acceleration in the *x*-direction, L/t^2.
g_y	gravitational acceleration in the *y*-direction, L/t^2.
H	variable defined in Eq. (15), 1/t.
I_1	modified Bessel function of the first kind of order one.
J_1	Bessel function of the first kind of order one.
L_x	length of the aquifer, L.
M_{in}	injected mass, M.
M_δ	mass injected "instantaneously" over the porous medium cross-sectional area, M/L^2.
M_c	mass of colloids, M_c.
M_s	mass of the solid matrix, M_s.
$r_{c-c*^{(i)}}$	rate coefficient of irreversible colloid attachment onto the sold matrix, 1/t.
$r_{c-c*^{(r)}}$	rate coefficient of reversible colloid attachment onto the sold matrix, 1/t.
$r_{c*^{(r)}-c}$	rate coefficient of reversible colloid detachment from the solid matrix, 1/t.
t	time, t.
t_p	time period during which the source concentration is constant, t.
U	interstitial velocity, L/t.
U_{tot}	total velocity (sum of average interstitial velocity with settling velocity), L/t.
U_s	restricted settling velocity, L/t.
$U_{s(x)}$	*x*-directional component of the restricted settling velocity, L/t.
x	Cartesian coordinate in the longitudinal direction, L.

Greek letters

β	angle of the main flow direction (*x*-direction) with respect to the horizontal direction.
ε	empirical correction factor, (–).
δ	Dirac delta function, 1/L.
ζ	dummy integration variable, t.
θ	porosity of the column material, (L^3 voids)/(L^3 solid matrix).
μ_w	dynamic viscosity of water, M/(L•t).
ξ	dummy integration variable, t.
ρ_b	bulk density of the solid matrix, M_s/L^3.
ρ_p	particle density, M/L^3.
ρ_w	fluid density, M/L^3.
τ	dummy integration variable, t.

models that account for attachment with two-site kinetics (Basha and Culligan, 2010).

The purpose of the current study is to present new analytical solutions to colloid transport models that account for attachment with two-site kinetics, instantaneous or broad pulse sources, and non-negligible gravity effects. To our best of knowledge there are no analytical solutions available in the literature for mathematical two-site models for dense colloids. Analytical models such as these may be a useful for the evaluation of conventional numerical models.

2. Mathematical formulation

2.1. Colloid mathematical model with reversible attachment

The transport of suspended colloid particles in one-dimensional, saturated, homogeneous porous media with uniform flow, accounting for combined nonequilibrium reversible and irreversible attachment onto the solid matrix along with gravity effects, is governed by the following partial differential equation (Chrysikopoulos and Syngouna, 2014)

$$\frac{\partial C_c(t,x)}{\partial t}+\frac{\rho_b}{\theta}\frac{\partial C_{c*}(t,x)}{\partial t}=D_c\frac{\partial^2 C_c(t,x)}{\partial x^2}-U\frac{\partial C_c(t,x)}{\partial x}-U_{s(x)}\frac{\partial C_c(t,x)}{\partial x} \quad (1)$$

where C_c [M_c/L^3] is the concentration of colloids (where M_c represents the mass of colloids); C_{c^*} [M_c/M_s] (where M_s represents the mass of the solid matrix) is the concentration of colloids attached onto the solid matrix; t [t] is time; x [L] is a Cartesian coordinate in the longitudinal direction; ρ_b [M_s/L^3] is the bulk density of the solid matrix; θ [–] is the porosity of the porous medium; D_c [L^2/t] is the longitudinal hydrodynamic dispersion coefficient of the suspended colloids; U [L/t] is the average interstitial velocity along the *x*-direction; $U_{s(x)}$ [L/t] is the *x*-directional component of the "restricted particle" settling velocity, U_s, which is just a modification of the "free particle" settling velocity, commonly used in static water columns (Russel et al., 1989), applicable to granular porous media (Chrysikopoulos and Syngouna, 2014):

$$U_{s(x)}=-f_s\frac{(\rho_p-\rho_w)d_p^2}{18\mu_w}g_x \quad (2)$$

where f_s [–] is the correction factor accounting for particle settling in the presence of a solid matrix of granular porous media; ρ_p [M/L^3] is the density of the colloid particle; ρ_w [M/L^3] is the density of the suspending fluid (water); μ_w [M/(L•t)] is the dynamic viscosity of water; d_p [L] is the colloid particle diameter; and g_x [L/t^2] is the *x*-directional gravity component defined as:

$$g_x=g\sin\beta \quad (3)$$

where g [L/t^2] is the gravity acceleration; β [°] is the angle of the main flow direction (*x*-direction) with respect to the horizontal direction ($-90^\circ \le \beta \le 90^\circ$) (see Fig. 1). The correction factor, f_s, is expressed as follows (Wan et al., 1995):

$$f_s=\frac{b+0.67}{b+0.93/\varepsilon} \quad (4)$$

where b [–] ($b \approx 1$) is the average free settling segment length to the grain radius ratio, and ε [–] ($0 \le \varepsilon \le 1$) is an empirical correction factor that takes into account the effect of the grain surface. Note that granular porous media consisting of grains with smooth surfaces, do not provide additional frictional resistance, but only contribute to the tortuosity (Wan et al., 1995), and the value of the f_s coefficient can be set to $f_s \approx 0.9$. For simplicity purposes, the average interstitial velocity, U, and the settling velocity, $U_{s(x)}$, can be replaced by their sum (Chrysikopoulos and Syngouna, 2014):

$$U_{tot}=U+U_{s(x)} \quad (5)$$

The concentration of colloids attached onto the solid matrix, C_{c^*}, is assumed to be a combination of reversibly, $C_{c*}^{(r)}$ [M_c/M_s], and irreversibly, $C_{c*}^{(i)}$ [M_c/M_s], attached colloids (Katzourakis and Chrysikopoulos, 2014):

$$C_{c*}=C_{c*}^{(r)}+C_{c*}^{(i)} \quad (6)$$

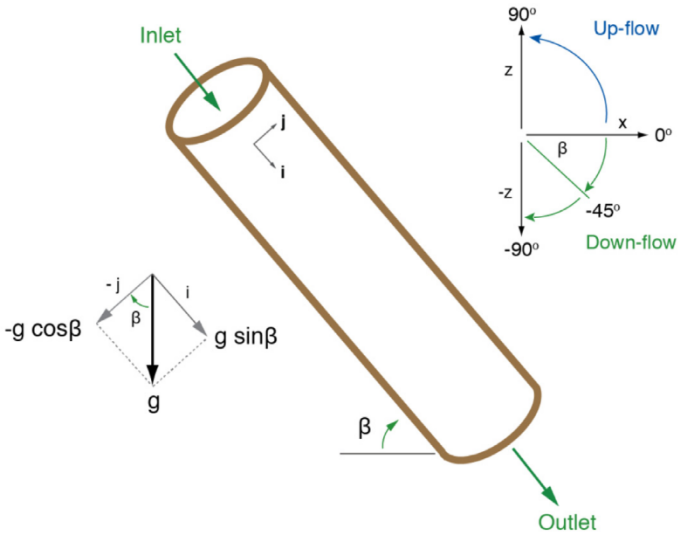

Fig. 1. A porous medium with down-flow velocity. The velocity orientation is: $+i$, and the gravity vector components are: $g_x = g\ \sin\beta$, and $g_y = -g\ \cos\beta$.

Consequently, the accumulation term in Eq. (1) can be expressed as:

$$\frac{\rho_b}{\theta}\frac{\partial C_{c*}(t,x)}{\partial t} = \frac{\rho_b}{\theta}\left[\frac{\partial C_{c*}^{(r)}(t,x)}{\partial t} + \frac{\partial C_{c*}^{(i)}(t,x)}{\partial t}\right] \tag{7}$$

The reversible accumulation term is given by (Sim and Chrysikopoulos, 1998, 1999):

$$\frac{\rho_b}{\theta}\frac{\partial C_{c*}^{(r)}(t,x)}{\partial t} = r_{c-c*(r)} C_c(t,x) - r_{c*(r)-c}\frac{\rho_b}{\theta} C_{c*}^{(r)}(t,x) \tag{8}$$

where $r_{c-c*(r)}$ [1/t] is the forward rate coefficient of colloid attachment onto the solid matrix, and $r_{c*(r)-c}$ [1/t] is the reverse rate coefficient of colloid detachment from the solid matrix. The irreversible accumulation term is given by (Compère et al., 2001):

$$\frac{\rho_b}{\theta}\frac{\partial C_{c*}^{(i)}(t,x)}{\partial t} = r_{c-c*(i)} C_c(t,x) \tag{9}$$

where $r_{c-c*(i)}$ is the forward rate coefficient of irreversible colloid attachment onto the solid matrix. Note that for both reversible and irreversible accumulation terms Eqs. (8) and (9) the rate of attachment is assumed to be linear (blocking or ripening effects are neglected). Substituting Eqs. (5) and (7)–(9) in the colloid transport Eq. (1) yields the following partial differential equation:

$$\frac{\partial C_c(t,x)}{\partial t} = D_c\frac{\partial^2 C_c(t,x)}{\partial x^2} - U_{tot}\frac{\partial C_c(t,x)}{\partial x} - \left[r_{c-c*(r)} + r_{c-c*(i)}\right] C_c(t,x) + r_{c*(r)-c}\frac{\rho_b}{\theta} C_{c*}^{(r)}(t,x) \tag{10}$$

An expression for the reversible attached colloid concentration $C_{c*}^{(r)}$ in terms of C_c can be found from the solution of (8) subject to the initial condition of zero attached colloid concentration ($C_c(0,x) = 0$) as follows:

$$C_{c*}^{(r)}(t,x) = r_{c-c*(r)}\frac{\theta}{\rho_b}\int_0^t C_c(\tau,x)\exp\left[-r_{c*(r)-c}(t-\tau)\right]d\tau \tag{11}$$

where τ is a dummy integration variable. Substituting (11) into (10) yields the governing two-site, one-dimensional colloid transport equation with combined reversible and irreversible attachment:

$$\frac{\partial C_c(t,x)}{\partial t} = D_c\frac{\partial^2 C_c(t,x)}{\partial x^2} - U_{tot}\frac{\partial C_c(t,x)}{\partial x} - A C_c(t,x) - B\int_0^t C_c(\tau,x)\exp\left[-H(t-\tau)\right]d\tau \tag{12}$$

where the following definitions were used:

$$A = r_{c-c*(r)} + r_{c-c*(i)} \tag{13}$$

$$B = -r_{c-c*(r)} r_{c*(r)-c} \tag{14}$$

$$H = r_{c*(r)-c} \tag{15}$$

2.2. Initial and boundary conditions

The initial condition and the appropriate boundary conditions for colloids, written for one-dimensional semi-infinite porous medium are as follows (Sim and Chrysikopoulos, 1995; Thomas and Chrysikopoulos, 2007):

$$C_c(0,x) = 0 \tag{16}$$

$$\frac{\partial C_c(t,\infty)}{\partial x} = 0 \tag{17}$$

$$-D_c\frac{\partial C_c(t,0)}{\partial x} + U C_c(t,0) = \begin{cases} U C_{c_0}, & t \le t_p \\ 0, & t > t_p \end{cases} \tag{18}$$

$$-D_c\frac{\partial C_c(t,0)}{\partial x} + U C_c(t,0) = M_\delta\delta(t) \tag{19}$$

where $\mathbf{M}_\delta = M_{in}/A_c\theta$ [M_c/L^2] is the mass injected "instantaneously" over the cross-sectional area of the porous medium (where M_{in} [M_c] is the injected mass and A_c [L^2] is the cross sectional area of the porous medium); C_{c_0} [M_c/L^3] is the injected constant concentration of colloids; t_p [t] is a fixed period of time during which the source concentration remains constant and $\delta(t)$ [1/t] is the Dirac delta function:

$$\delta(t) = \begin{cases} 0 & t \neq 0 \\ 1 & t = 0 \end{cases} \quad \& \quad \int_{-\infty}^{+\infty}\delta(t)dt = 1 \tag{20}$$

The condition (16) establishes that there is no initial concentration of colloids within the porous medium. The downstream condition (17) preserves concentration continuity (Chrysikopoulos et al., 1990b). The upstream Eqs. (18) and (19) define the way colloids are introduced into the aquifer. The condition (18) refers to a continuous source that provides constant concentration of colloids over a broad pulse, which is a predefined time period t_p (Sim and Chrysikopoulos, 1995). Whereas, Eq. (19) refers to instantaneous injection of colloids with total injected mass equal to M_{in}.

3. Analytical solutions

3.1. Analytical solution for colloids with instantaneous source

The analytical solution for the two-site colloid transport Eq. (12) subject to initial and boundary conditions (16), (17) and (19) was obtained using Laplace transforms by following the work of Chrysikopoulos et al. (1990a) and Sim and Chrysikopoulos (1998, 1999). The resulting solution is:

$$C_c(t,x) = \frac{M_\delta}{D_c^{1/2}}exp\left[\frac{U_{tot}x}{2D_c} - Ht\right] \times\left\{\frac{1}{(\pi t)^{1/2}}exp\left[\frac{-x^2}{4D_c t} + \left(H - A - \frac{U_{tot}^2}{4D_c}\right)t\right] - \frac{U_{tot}}{2D_c^{1/2}}exp\left[\frac{U_{tot}x}{2D_c} + (H-A)t\right] \times erfc\left[\frac{x}{2(D_c t)^{1/2}} + \frac{U_{tot}}{2}\left(\frac{t}{D_c}\right)^{1/2}\right]\right\} - \int_0^t \frac{B\zeta}{\{B\zeta(t-\zeta)\}^{1/2}}J_1\left[2(B\zeta(t-\zeta))^{1/2}\right]$$

Table 1
Parameters for the transport experiments in horizontal columns ($\beta = 0°$).

Clay type:		KGa-1		STx-1b	
Parameter	Status	Exp. 1	Exp. 2	Exp. 1	Exp. 2
D_c (cm^2/min)	Fitted	0.99 ± 0.3	0.25 ± 0.1	0.34 ± 0.1	0.4 ± 0.1
$r_{c-c*^{(r)}}$ (1/min)	VC[a]	0.006	0.045	0.013	0.047
$r_{c*^{(r)}-c}$(1/min)	Fitted	0.022 ± 0.01	0.135 ± 0.04	0.0355 ± 0.01	0.13 ± 0.01
$r_{c-c*^{(i)}}$ (1/min)	Fitted	0.014 ± 0.002	0.03 ± 0.01	0.018 ± 0.002	0.043 ± 0.01
U (cm/min)	SC[b]	0.74	1.21	0.74	1.21
θ (-)	SC[b]	0.42	0.42	0.42	0.42
t_p (min)	SC[b]	117.0	75.0	119.0	75.5
C_{c_0} (mg/mL)	SC[b]	69.1	63.8	91.2	87.6
L_x (cm)	SC[b]	30	30	30	30

[a] VC – (Vasiliadou and Chrysikopoulos, 2011).
[b] SC – (Syngouna and Chrysikopoulos, 2012).

$$\times\left\{\frac{1}{(\pi\zeta)^{1/2}}exp\left[\frac{-x^2}{4D_c\zeta}+\left(H-A-\frac{U_{tot}{}^2}{4D_c}\right)\zeta\right]-\frac{U_{tot}}{2D_c{}^{1/2}}exp\left[\frac{U_{tot}x}{2D_c}+(H-A)\zeta\right]\times erfc\left[\frac{x}{2(D_c\zeta)^{1/2}}+\frac{U_{tot}}{2}\left(\frac{\zeta}{D_c}\right)^{1/2}\right]\right\}d\zeta\Bigg\} \quad (21)$$

where J_1 is the Bessel function of the first kind of order one; "exp" is the exponential function; and "erfc" is the complementary error function, ζ is a dummy integration variable. In order to evaluate the above analytical solution for the special case of $B<0$, the following relationship can be employed (Abramowitz and Stegun, 1964):

$$J_1(ix) = i \cdot I_1(x) \quad (22)$$

where I_1 is the modified Bessel function of the first kind of order one. Therefore, the term $J_1[2\{B\zeta(t-\zeta)\}^{1/2}]/\{B\zeta(t-\zeta)\}^{1/2}$ can be replaced by $-I_1[2\{|B\zeta(t-\zeta)|\}^{1/2}]/\{|B\zeta(t-\zeta)|\}^{1/2}$.

3.2. Analytical solution for colloids with broad pulse source

The analytical solution for the two-site colloid transport Eq. (12) subject to initial and boundary conditions (16)–(18), was obtained using Laplace transforms in a fashion similar to the case of instantaneous source to yield:

$$C_c(t,x)=\begin{cases}\Omega(t,x) & 0<t\le t_p\\ \Omega(t,x)-\Omega(t-t_p,x) & t>t_p\end{cases} \quad (23)$$

where

$$\Omega(t,x)=\frac{C_{c_0}U_{tot}}{D_c^{1/2}}\exp\left[\frac{U_{tot}x}{2D_c}\right]\Bigg\{\int_0^t\int_0^\tau He^{-H\tau}J_0\left[2(B\xi(\tau-\xi))^{1/2}\right]\cdot\Bigg\{\frac{1}{(\pi\xi)^{1/2}}\exp\left[\frac{-x^2}{4D_c\xi}+\left(H-A-\frac{U_{tot}{}^2}{4D_c}\right)\xi\right]-\frac{U_{tot}}{2D_c^{1/2}}\exp\left[\frac{U_{tot}x}{2D_c}+(H-A)\xi\right]\cdot erfc\left[\frac{x}{2(D_c\xi)^{1/2}}+\frac{U_{tot}}{2}\left(\frac{\xi}{D_c}\right)^{1/2}\right]\Bigg\}d\xi d\tau+e^{-Ht}\int_0^t J_0\left[2(B\xi(t-\xi))^{1/2}\right]\cdot\Bigg\{\frac{1}{(\pi\xi)^{1/2}}\exp\left[\frac{-x^2}{4D_c\xi}+\left(H-A-\frac{U_{tot}{}^2}{4D_c}\right)\xi\right]-\frac{U_{tot}}{2D_c^{1/2}}\exp\left[\frac{U_{tot}x}{2D_c}+(H-A)\xi\right]\cdot erfc\left[\frac{x}{2(D_c\xi)^{1/2}}+\frac{U_{tot}}{2}\left(\frac{\xi}{D_c}\right)^{1/2}\right]\Bigg\}d\xi\Bigg\} \quad (24)$$

4. Model simulations and application to experimental data

The performance of the two-site analytical solution for broad pulse source (23) and (24) was illustrated by fitting the experimental data collected by Syngouna and Chrysikopoulos (2013), who have conducted transport experiments with two clays kaolinite (KGa-1b) and montmorillonite (STx-1b), in horizontal columns packed with glass beads under two different flow rates ($Q = 1.5$ and 2.5 mL/min). The fitting of the experimental data was achieved with the autonomous multipurpose fitting software, ColloidFit (Katzourakis and Chrysikopoulos, 2017). Only the parameters D_c, $r_{c-c*^{(i)}}$ and $r_{c*^{(r)}-c}$ were fitted, while the parameter value for $r_{c-c*^{(r)}}$ was obtained from the literature (Vasiliadou and Chrysikopoulos, 2011). The fitted parameters along with the corresponding 95% confidence levels are listed in Table 1. The experimental normalized breakthrough concentrations and the respective best-fitted model simulations are presented in Fig. 2. For both flow rates considered here, the analytical solution (23) and (24) successfully simulated the KGa-1b and STx-1b breakthrough data. Undoubtedly, the two-site model effectively described the transport of the available experimental data.

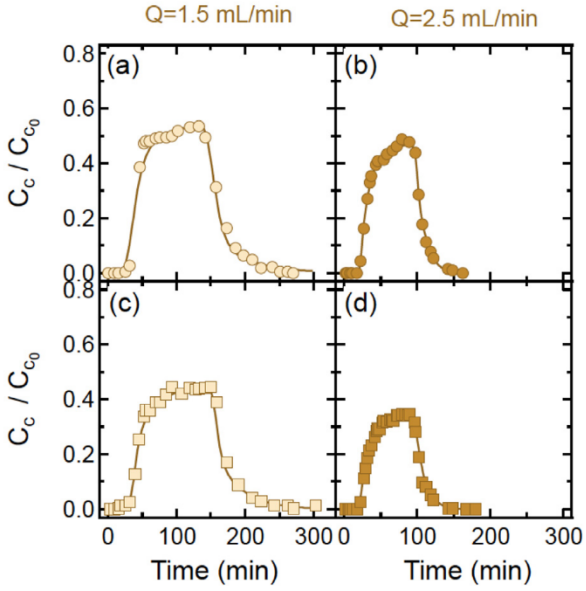

Fig. 2. Normalized breakthrough experimental data (symbols) collected by Syngouna and Chrysikopoulos (2013) for the transport of two clays in a horizontal column packed with glass beads under two different flow rates, together with the best fitted model simulations (solid curves). Here: (a,b) KGa-1b (circles), and (c,d) STx-1b (squares).

Table 2
Parameters for model simulations.

Parameter	Values	References
D_c (cm^2/min)	0.5	(Schulze-Makuch, 2005)
$r_{c-c^{*(i)}}$ (1/min)	0.013	This work
$r_{c^{*(i)}-c}$ (1/min)	0.02	This work
$r_{c-c^{*(i)}}$ (1/min)	0.0002	–
U (cm/min)	3.33×10^{-2}	(Chrysikopoulos et al., 2012)
U_s (cm/min)	6.68×10^{-3}	Eq. (2)
U_{tot} (cm/min)	4.0×10^{-2} (for $\beta = -90°$) 2.66×10^{-2} (for $\beta = 90°$)	Eq. (5)
θ (-)	0.42	(Syngouna and Chrysikopoulos, 2012)
L_x (cm)	30	–
Broad pulse source		
t_p (min)	6000	–
C_{c_0} (mg/mL)	1	–
Instantaneous source		
M_{in} (mg)	1	–
A_c (cm^2)	4.9	–

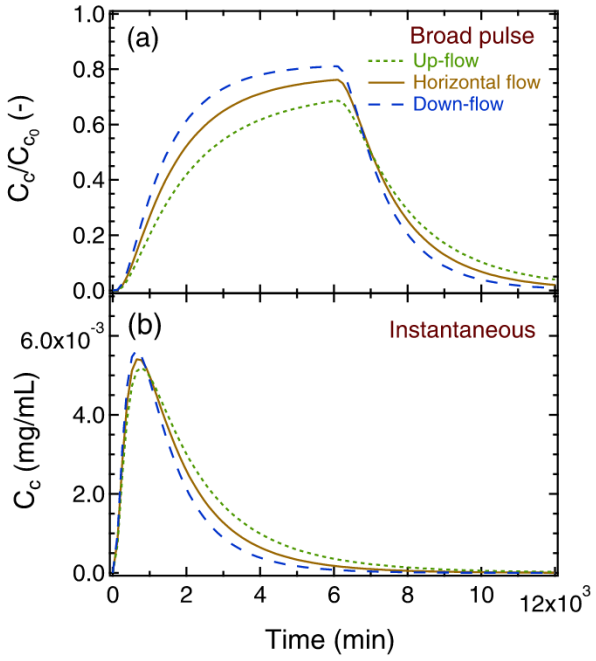

Fig. 3. Time history of model simulated normalized concentrations for: (i) vertical up-flow (dotted line), (ii) horizontal flow (solid line), and (iii) vertical down-flow (dashed line). Here t_p = 6000 min for the broad pulse case and M_{in} = 1 mg for the instantaneous case.

To illustrate how gravity effects associated with dense colloids can affect colloid transport, simulations were performed under vertical up, vertical down and horizontal flow conditions for both instantaneous source (21) and broad pulse source (23) and (24) analytical solutions. The colloids were assumed to be spherical with diameter d_p = 1.4 μm and density $\rho_p = 2.2 \times 10^{-3}$ kg/cm^3. Additionally, the "restricted particle" settling velocity of the dense colloids was estimated with Eq. (2) equal to $U_s = 6.68 \times 10^{-3}$ cm/min, using $\mu_w = 6 \times 10^{-4}$ kg/(cm min), $\rho_w = 9.98 \times 10^{-4}$ kg/cm^3, f_s = 0.9 (Wan et al., 1995), and $g = 3.53 \times 10^6$ cm/min^2. All parameter values required for the simulations are listed in Table 2. The simulated breakthrough curves are shown in Fig. 3. Clearly, vertical down flow leads to increased average velocity, whereas vertical up flow leads to decreased average velocity compared to horizontal flow. Larger velocities allow faster exit of colloid particles from the porous medium. The effects of gravity are more pronounced for the broad pulse source rather than the instantaneous source. Note that at later times ($t > t_p$ = 6000 min), colloid particle concentrations for the broad pulse source case are lower for down flow than up flow conditions.

To further illustrate the model sensitivity to the various model parameters, numerous simulations were performed for several coefficient values for both broad pulse and instantaneous cases. The simulations using the analytical solution for instantaneous source (21) are presented in Fig. 4, and for broad pulse source (23) and (24) are presented in Fig. 5. For each model parameter four simulations were conducted for a horizontal porous medium with length L_x = 30 cm. The injected mass was M_{in} = 1 mg for the instantaneous case, whereas the source release time period for the broad pulse case was t_p = 6000 min. All other required parameter values are listed in Table 2. It is apparent from Figs. (4) and (5) that the simulations for both instantaneous and broad pulse source cases exhibit similar behavior. Colloid concentrations exhibit higher peaks as the values for parameters D_c, $r_{c-c*(r)}$ and $r_{c-c*(i)}$ decrease and higher peaks as the value of $r_{c*(r)-c}$ increases. As expected, lower values of the hydrodynamic dispersion coefficient D_c lead to reduced particle spreading, which in turn leads to sharper concentration peaks, slower breakthrough times, and reduced late time concentrations (see Figs. 4(a) and 5(a)). Similarly, lower values of the rates $r_{c-c*(r)}$ and $r_{c-c*(i)}$ decrease colloid attachment on the solid matrix and consequently lead to higher concentration peaks (see Figs. 4(b),(d), 5(b) and (d)). Finally, higher values of the rate $r_{c*(r)-c}$ increase colloid detachment from the solid matrix and consequently cause higher colloid concentration peaks (see Figs. 4(c) and 5(c)).

Finally, the analytical solutions developed in this study, were compared against two software packages. The first comparison was between the simplified one-site reversible ($r_{c-c*(i)}$ = 0 [1/min]), broad pulse model of this study for a horizontal column (β = 0°, U_{tot} = 0.0333 [cm/min]) with the Stanmod software package (Simunek et al., 1999; van Genuchten et al., 2012), as illustrated in Fig. 6(a). The second comparison was between the complete two-site reversible and irreversible ($r_{c-c*(i)}$ = 0.0002 [1/min]) broad pulse model of this study for a vertical column with flow in the vertical down direction (β = −90°, U_{tot}=0.04 [cm/min]) and the well-known Comsol Multiphysics^{TM} software package (see Fig. 6(b)). The model parameters used for both comparisons are listed in Table 2. Clearly, the results presented in Fig. 6 for both comparisons are excellent.

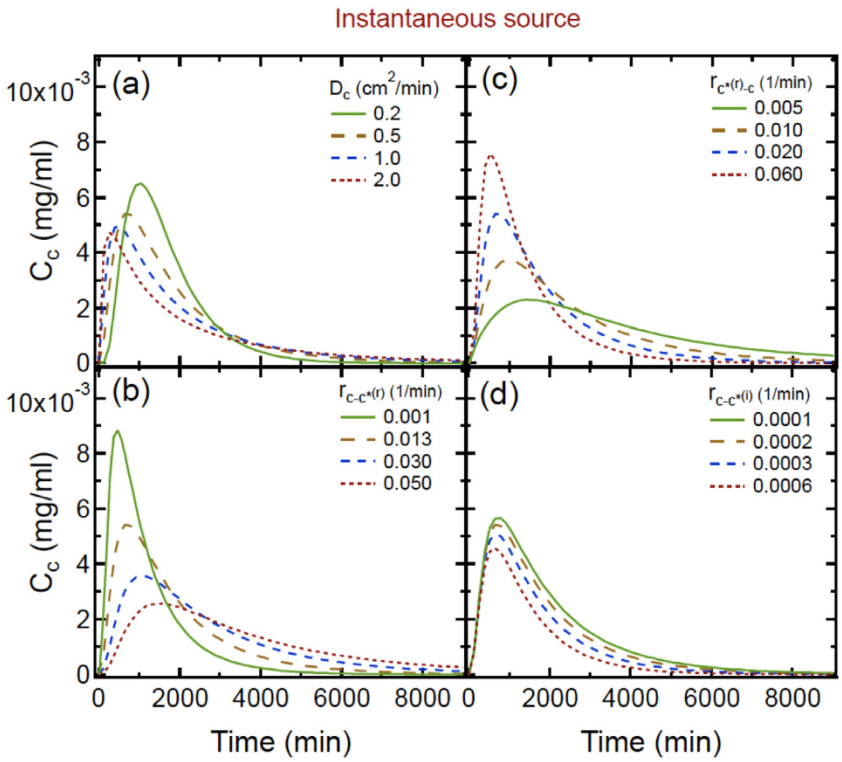

Fig. 4. Sensitivity analysis simulations for: (a) hydrodynamic dispersion, D_c, (b) reversible colloid attachment rate, $r_{c-c^{*(r)}}$, (c) reversible colloid detachment rate, $r_{c^{*(r)}-c}$, and (d) irreversible colloid attachment rate, $r_{c-c^{*(i)}}$. Here the instantaneously injected mass is M_{in} =1 mg.

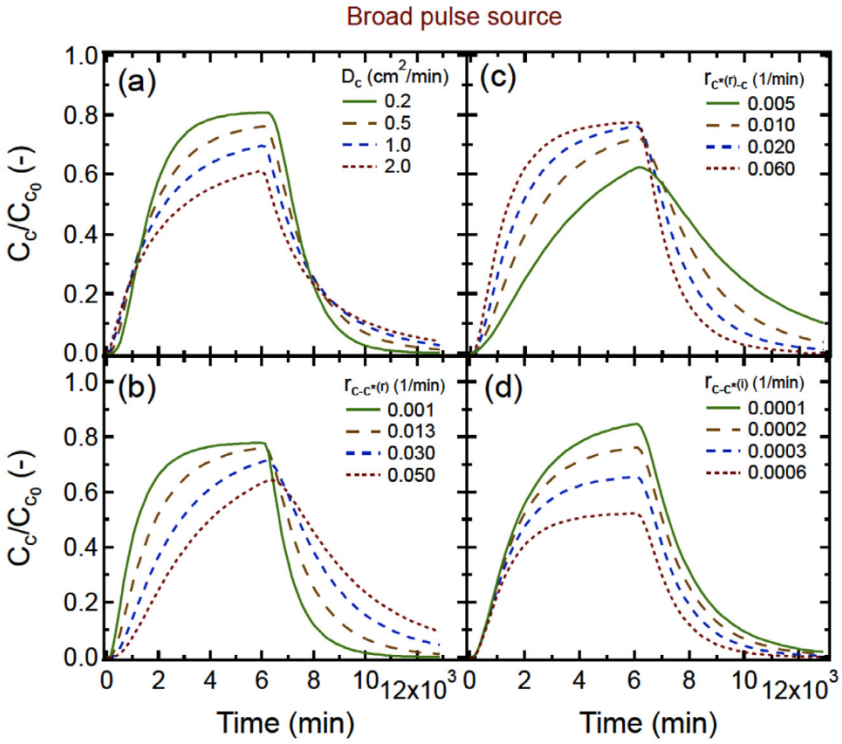

Fig. 5. Sensitivity analysis simulations for: (a) hydrodynamic dispersion, D_c, (b) reversible colloid attachment rate $r_{c-c^{*(r)}}$, (c) reversible colloid detachment rate, $r_{c^{*(r)}-c}$, and (d) irreversible colloid attachment rate $r_{c-c^{*(i)}}$. Here the broad pulse source release time period is t_p = 6000 min.

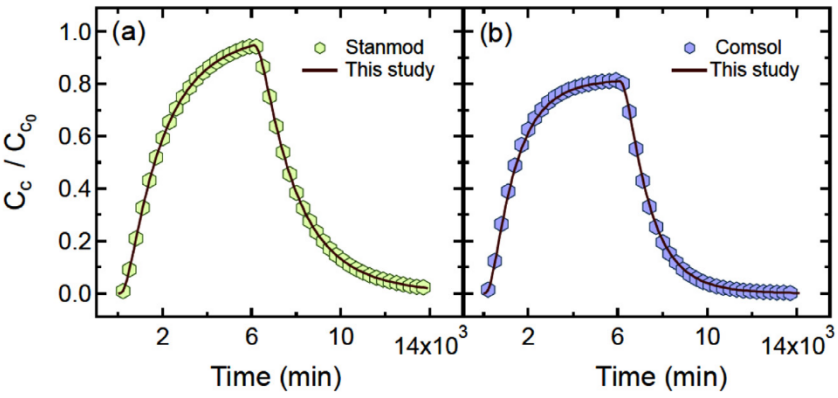

Fig. 6. Comparison of the analytical broad pulse model with: (a) Stanmod software package (U_{tot} = 0.0333 [cm/min], $r_{c-c*(i)}$ = 0 [1/min]), and (b) Comsol software package (U_{tot} = 0.04 [cm/min], $r_{c-c*(i)}$ = 0.0002 [1/min]). All other required parameter values are listed in Table 2.

5. Summary and conclusions

Analytical solutions for dense colloid transport in one-dimensional, water saturated porous media were presented. Colloid particles were assumed to be either suspended in the aqueous phase or attached reversibly and/or irreversibly onto the solid matrix. The new analytical solutions presented here account for both instantaneous and broad pulse sources. Model simulations have shown that gravity can influence colloid transport by either enhancing or hindering their migration, depending on the flow direction. The new two-site analytical solution for broad pulse source configuration reported here, successfully fitted available experimental data. Sensitivity analysis showed that the analytical solutions for both instantaneous and broad pulse sources follow similar trends. Finally, a simplified form of the analytical model developed in this study was successfully compared to other existing solutions that neglect the effects of gravity.

Acknowledgements

This research did not receive any specific grant from funding agencies in the public, commercial, or not-for-profit sectors.

References

Abramowitz, M., Stegun, I.A., 1964. Handbook of mathematical functions with formulas, graphs and mathematical tables. J. Appl. Mech..

Anders, R., Chrysikopoulos, C.V., 2009. Transport of viruses through saturated and unsaturated columns packed with sand. Transp. Porous Media 76, 121–138. https://doi.org/10.1007/s11242-008-9239-3.

Basha, H.A., Culligan, P.J., 2010. Modeling particle transport in downward and upward flows. Water Resour. Res. 46. https://doi.org/10.1029/2009WR008133.

Bradford, S.A., Torkzaban, S., Simunek, J., 2011. Modeling colloid transport and retention in saturated porous media under unfavorable attachment conditions. Water Resour. Res. 47. https://doi.org/10.1029/2011WR010812.

Cameron, D.R., Klute, A., 1977. Convective-dispersive solute transport with a combined equilibrium and kinetic adsorption model. Water Resour. Res. 13 (1), 183–188.

Chrysikopoulos, C.V., Katzourakis, V.E., 2015. Colloid particle size-dependent dispersivity. Water Resour. Res. 51, 4668–4683. https://doi.org/10.1002/2014WR016094.

Chrysikopoulos, C.V., Kitanidis, P., Roberts, P., 1990a. Analysis of one-dimensional solute transport through porous media with spatially variable retardation factor. Water Resour. Res. 26, 437–446. https://doi.org/10.1029/WR026i003p00437.

Chrysikopoulos, C.V., Roberts, P.V., Kitanidis, P.K., 1990b. One-dimensional solute transport in porous media with partial well-to-well recirculation: application to field experiments. Water Resour. Res. 26, 1189–1195. https://doi.org/10.1029/WR026i006p01189.

Chrysikopoulos, C.V., Syngouna, V.I., 2014. Effect of gravity on colloid transport through water-saturated columns packed with glass beads: modeling and experiments. Environ. Sci. Technol. 48, 6805–6813. https://doi.org/10.1021/es501295n.

Chrysikopoulos, C.V., Syngouna, V.I., Vasiliadou, I.A., Katzourakis, V.E., 2012. Transport of Pseudomonas putida in a 3-D Bench Scale Experimental Aquifer. Transp. Porous Media 94, 617–642. https://doi.org/10.1007/s11242-012-0015-z.

Compère, F., Porel, G., Delay, F., 2001. Transport and retention of clay particles in saturated porous media. Influence of ionic strength and pore velocity. J. Contam. Hydrol. 49, 1–21. https://doi.org/10.1016/S0169-7722(00)00184-4.

Flowers, T.C., Hunt, J.R., 2007. Viscous and gravitational contributions to mixing during vertical brine transport in water-saturated porous media. Water Resour. Res. 43. n/a–n/a https://doi.org/10.1029/2005WR004773 .

Ginn, T.R., Wood, B.D., Nelson, K.E., Scheibe, T.D., Murphy, E.M., Clement, T.P., 2002. Processes in microbial transport in the natural subsurface. Adv. Water Resour.. https://doi.org/10.1016/S0309-1708(02)00046-5.

Harvey, R.W., Garabedlan, S.P., 1991. Use of colloid filtration theory in modeling movement of bacteria through a contaminated sandy aquifer. Environ. Sci. Technol. 25, 178–185. https://doi.org/10.1021/es00013a021.

James, S.C., Chrysikopoulos, C.V., 2003. Analytical solutions for monodisperse and polydisperse colloid transport in uniform fractures. Colloids Surf. A Physicochem. Eng. Asp. 226, 101–118. https://doi.org/10.1016/S0927-7757(03)00316-9.

Katzourakis, V.E., Chrysikopoulos, C.V., 2017. Fitting the Transport and Attachment of Dense Biocolloids in One-Dimensional Porous Media: colloidFit. Groundwater. https://doi.org/10.1111/gwat.12501.

Katzourakis, V.E., Chrysikopoulos, C.V., 2015. Modeling dense-colloid and virus cotransport in three-dimensional porous media. J. Contam. Hydrol. 181, 102–113. https://doi.org/10.1016/j.jconhyd.2015.05.010.

Katzourakis, V.E., Chrysikopoulos, C.V., 2014. Mathematical modeling of colloid and virus cotransport in porous media: application to experimental data. Adv. Water Resour. 68, 62–73. https://doi.org/10.1016/j.advwatres.2014.03.001.

Keller, A.A., Sirivithayapakorn, S., Chrysikopoulos, C.V., 2004. Early breakthrough of colloids and bacteriophage MS2 in a water-saturated sand column. Water Resour. Res. 40. https://doi.org/10.1029/2003WR002676.

Lee, K.Y., Chrysikopoulos, C.V., 2002. Dissolution of a well-defined trichloroethylene pool in saturated porous media: experimental results and model simulations. Water Res.. https://doi.org/10.1016/S0043-1354(02)00097-0.

Park, N., Blanford, T.N., Huyakorn, P.S., 1992. VIRALT: A Modular Semi-Analytical and Numerical Model for Simulating Viral Transport in Ground Water. Int. Gr. Water Model. Center, Golden, CO.

Russel, W.B., Saville, D.A., Schowalter, W.R., 1989. Colloidal Dispersions. Cambridge University Press.

Saiers, J.E., Hornberger, G.M., Liang, L., 1994. First- and second-order kinetics approaches for modeling the transport of colloidal particles in porous media. Water Resour. Res.. https://doi.org/10.1029/94WR01046.

Schijven, J.F., Hassanizadeh, S.M., De Bruin, R.H.A.M., 2002. Two-site kinetic modeling of bacteriophages transport through columns of saturated dune sand. J. Contam. Hydrol.. https://doi.org/10.1016/S0169-7722(01)00215-7.

Scholl, M.A., Harvey, R.W., 1992. Laboratory investigations on the role of sediment surface and groundwater chemistry in transport of bacteria through a contaminated sandy aquifer. Environ. Sci. Technol.. https://doi.org/10.1021/es00031a020.

Schulze-Makuch, D., 2005. Longitudinal dispersivity data and implications for scaling behavior. Ground Water.. https://doi.org/10.1111/j.1745-6584.2005.0051.x.

Shellenberger, K., Logan, B.E., 2002. Effect of molecular scale roughness of glass beads on colloidal and bacterial deposition. Environ. Sci. Technol.. https://doi.org/10.1021/es015515k.

Sim, Y., Chrysikopoulos, C., 1998. Three-dimensional analytical models for virus transport in saturated porous media. Transp. Porous Media 30, 87–112. https://doi.org/10.1023/A:1006596412177.

Sim, Y., Chrysikopoulos, C., 1996. Analytical models for one-dimensional virus transport in saturated porous media (vol 31, pg 1429, 1995). Water Resour. Res. 32, 2607–2611. https://doi.org/10.1029/96wr00675.

Sim, Y., Chrysikopoulos, C.V., 1999. Analytical solutions for solute transport in saturated porous media with semi-infinite or finite thickness. Adv. Water Resour. 22, 507–519. https://doi.org/10.1016/S0309-1708(98)00027-X.

Sim, Y., Chrysikopoulos, C.V., 1995. Analytical models for one-dimensional virus transport in saturated porous media. Water Resour. Res. 31, 1429–1437. https://doi.org/10.1029/95WR00199.

Šimůnek, J., van Genuchten, M.Th., Šejna, M., Toride, N., Leij, F.J., 1999. The STANMOD computer software for evaluating solute transport in porous media using analytical solutions of convection-dispersion equation. Versions 1.0 and 2.0. IGWMC - TPS - 71, 32. International Ground Water Modeling Center, Colorado School of Mines, Golden, Colorado.

Syngouna, V.I., Chrysikopoulos, C.V., 2016. Cotransport of clay colloids and viruses through water-saturated vertically oriented columns packed with glass beads: gravity effects. Sci. Total Environ. 545–546, 210–218. https://doi.org/10.1016/j.scitotenv.2015.12.091.

Syngouna, V.I., Chrysikopoulos, C.V., 2015. Experimental investigation of virus and clay particles cotransport in partially saturated columns packed with glass beads. J. Colloid Interface Sci. 440, 140–150. https://doi.org/10.1016/j.jcis.2014.10.066.

Syngouna, V.I., Chrysikopoulos, C.V., 2013. Cotransport of clay colloids and viruses in water saturated porous media. Colloids Surf. A Physicochem. Eng. Asp. 416, 56–65. https://doi.org/10.1016/j.colsurfa.2012.10.018.

Syngouna, V.I., Chrysikopoulos, C.V., 2012. Transport of biocolloids in water saturated columns packed with sand: effect of grain size and pore water velocity. J. Contam. Hydrol. 129–130, 11–24. https://doi.org/10.1016/j.jconhyd.2012.01.010.

Syngouna, V.I., Chrysikopoulos, C.V., Kokkinos, P., Tselepi, M.A., Vantarakis, A., 2017. Cotransport of human adenoviruses with clay colloids and TiO2nanoparticles in saturated porous media: effect of flow velocity. Sci. Total Environ. https://doi.org/10.1016/j.scitotenv.2017.04.082.

Tan, Y., Gannon, J.T., Baveye, P., Alexander, M., 1994. Transport of bacteria in an aquifer sand: experiments and model simulations. Water Resour. Res.. https://doi.org/10.1029/94WR02032.

Thomas, J.M., Chrysikopoulos, C.V., 2007. Experimental investigation of acoustically enhanced colloid transport in water-saturated packed columns. J. Colloid Interface Sci. https://doi.org/10.1016/j.jcis.2006.12.062.

Tong, M., Johnson, W.P., 2007. Colloid population heterogeneity drives hyperexponential deviation from classic filtration theory. Environ. Sci. Technol. 41, 493–499. https://doi.org/10.1021/es061202j.

Tong, M., Johnson, W.P., 2006. Excess colloid retention in porous media as a function of colloid size, fluid velocity, and grain angularity. Environ. Sci. Technol. https://doi.org/10.1021/es061201r.

Tufenkji, N., Elimelech, M., 2005. Breakdown of colloid filtration theory: role of the secondary energy minimum and surface charge heterogeneities. Langmuir 21, 841–852. https://doi.org/10.1021/la048102g.

Van Genuchten, M.T., Wagenet, R.J., 1989. Two-site/two-region models for pesticide transport and degradation: theoretical development and analytical solutions. Soil Sci. Soc. Am. J. 53 (5), 1303–1310.

van Genuchten, M.T., Šimůnek, J., Leij, F.L., Toride, N., Šejna, M., 2012. STANMOD: model use, calibration and validation, special issue Standard/Engineering Procedures for Model Calibration and Validation. Trans. ASABE 5 (4), 1353–1366.

Vasiliadou, I.A., Chrysikopoulos, C.V., 2011. Cotransport of *Pseudomonas putida* and kaolinite particles through water-saturated columns packed with glass beads. Water Resour. Res. 47. https://doi.org/10.1029/2010WR009560.

Wan, J.M., Tokunaga, T.K., Tsang, C.F., 1995. Bacterial Sedimentation through a Porous-Medium. Water Resour. Res. 31, 1627–1636.

Xu, S., Gao, B., Saiers, J.E., 2006. Straining of colloidal particles in saturated porous media. Water Resour. Res. 42.

Yoon, J.S., Germaine, J.T., Culligan, P.J., 2006. Visualization of particle behavior within a porous medium: mechanisms for particle filtration and retardation during downward transport. Water Resour. Res.. https://doi.org/10.1029/2004WR003660.